Compact Detector Modules for High Resolution PET Imaging with LYSO and Avalanche Photodiode Arrays

Martin Clajus, Victoria B. Cajipe, Robert F. Calderwood, Simon R. Cherry, Satoshi Hayakawa, Tümay O. Tümer, and Oded Yossifor

***Abstract*-- We have developed compact detector modules for high-resolution PET imaging. The modules consist of arrays of four by four 20 mm long LYSO crystals whose scintillation signals are read by avalanche photodiode arrays. The scintillator arrays are instrumented at both ends to facilitate depth-of-interaction determination by measuring the pulse-height ratio between the two ends of the LYSO crystal. To process the diode signals, we have developed a custom multi-channel integrated readout chip designed for excellent coincidence time resolution and low power dissipation. The IC offers various configuration options to allow for a high degree of flexibility in the design of the imaging system.**

I. Introduction

THE American Cancer Society estimates more than 215,000 new breast cancer diagnoses and more than 40,000 deaths from breast cancer in the United States in 2004 [1]. Mammography is a useful screening tool for detecting breast cancer, reducing mortality by about 25%, but is limited by a large number of false positive tests resulting in unnecessary biopsies and, more importantly, a considerable number of false negative tests resulting in missed diagnosis of cancer [2]. In the last few years it has become apparent that nuclear medicine techniques have the potential to play an important role in the diagnosis and treatment of patients with breast cancer [3,4]. Positron emission tomography (PET), using [^{18}F] fluoro-2-deoxy-D-glucose (FDG) as a tracer of tumor glucose metabolic activity, is an accurate, non-invasive imaging technology which probes tissue and organ function. This provides information which is complementary to the structural image obtained from mammography. Whole body PET is a well established technology, but it is expensive, and of limited availability. Furthermore, the typical spatial resolution of 8 – 16 mm is insufficient for accurate detection and imaging of smaller tumors. The extension of PET to small, more widely available, higher spatial resolution (< 3 mm) systems optimized for breast cancer imaging has the potential to save many lives. Several groups have therefore been exploring the design of dedicated breast imaging PET systems [5 – 11].

Detector modules based on planar-processed avalanche photodiode (APD) arrays and LYSO ($Lu_{1.8}Y_{0.2}SiO_5$) scintillator crystals can make these developments possible [12,13]. The APD arrays are available with 4 × 4 pixels and a 2.48 mm pitch or 8 × 8 pixels and a 1.27 mm pitch; the 2.48 mm pitch array which we work with here has a pixel active area of 2 × 2 mm^2, a gain of order 1000, and capacitance of 2.8 pF (excluding packaging) [14]. For room temperature operation, the leakage current is around 100 nA and the current noise is several $pA/\sqrt{Hz}$, when operated near maximum gain (for optimal timing resolution). The quantum efficiency is >60% at 420 nm, the peak emission wavelength of LYSO. Results of early measurements performed with LSO and a single channel APD of the same 2 × 2 mm^2 geometry and the same specifications were presented in [15].

The compact geometry and low mass of the APD arrays allow for double-ended readout of the LYSO crystals, to make depth of interaction (DOI) measurements, with the added engineering advantage of identical readout electronics for both sides of the crystal array. DOI measurement is critical to achieving a uniform spatial resolution in combination with high efficiency in an affordable instrument, with a ring diameter of about 20 to 30 cm. Another advantage of APDs is their relative insensitivity to magnetic fields, possibly enabling co-imaging with PET and NMR techniques in the future.

II. Overview of the Module Design

We have designed detector modules that take advantage of these developments by sandwiching a four-by-four array of LYSO scintillator crystals between two of the APD arrays discussed above. The crystal dimensions are 2 × 2 × 20 mm^3, with a 2.4 mm pitch between crystals to match the active area and pixel pitch of the APD arrays. To optimize DOI resolution, only the two crystal surfaces that face the APD arrays are

Manuscript received November 1 2004. This work was supported by the U.S. Department of Energy under Contract No. DE-FG03ER83058

M. Clajus, V.B. Cajipe, S. Hayakawa, and T.O. Tümer are with NOVA R&D, Inc., Riverside, CA 92507 USA (telephone: 951-781-7332, first author e-mail: martin.clajus@novarad.com).

R.F. Calderwood was with NOVA R&D, Inc., Riverside, CA 92507 USA. He is now with Integrated Circuits Design Concepts, Santa Ana, CA 92705 USA (telephone: 714-633-0455, e-mail: icdc@icdesignconcepts.com).

S.R. Cherry is with the Biomedical Engineering Department, University of California, Davis, CA 95616 USA (telephone: 530-754-9419, e-mail: srcherry@ucdavis.edu).

O. Yossifor is with Ocean Side Consulting, San Pedro, CA 90732 USA (telephone: 310-874-7735, e-mail: odedy@pacbell.net).

polished; all other surfaces are saw-cut. The space between the crystals is filled with optical epoxy loaded with barium sulfate reflector.

To read out these detector modules, we have developed a multi-channel readout IC optimized for high resolution APD/LYSO PET imaging. This chip, called FREDA (Fast Readout Electronics for Diode Arrays) has 64 channels, sufficient for instrumenting even the 8 × 8-pixel APD arrays with their finer position resolution. A high resolution PET scanner with DOI for breast cancer imaging can easily involve 5,000 – 20,000 channels, making excellent coincidence timing resolution essential in order to handle high event rates without significant background due to accidental coincidences. Given this large channel count, power dissipation is also a critical parameter. Since the avalanche gain in an APD is relatively low (compared to a typical PMT), sophisticated low-noise electronics must be placed close to the APDs. This further complicates the power dissipation issue, especially since the APD gain depends sensitively on temperature.

III. Chip Design Details

To address the requirements above, our chip design combines a high-speed, low-noise input amplifier with a constant-fraction discriminator (CFD). The CFD, especially when operated at the low thresholds permitted by the low amplifier noise, minimizes pulse-height dependent time walk and overall timing jitter that would degrade coincidence resolution. As shown in the top-level block diagram in Fig. 1, the IC provides on-chip circuitry to detect coincidences between the local discriminator outputs and the corresponding signals that are received from other chips in the system. For pulse-height measurements, each channel is equipped with shaper and peak/hold circuitry (cf. the channel block diagram in Fig. 2). The amplifier gains are digitally adjustable individually for each channel. When a coincidence trigger is generated, the peak of the shaper signal can be sampled and read out for any channel(s) the user selects. This flexibility permits DOI determination even in those cases where the smaller of the two scintillator signals involved is below or just barely above the discriminator threshold.

Fig. 3 shows the coincidence circuitry of the FREDA IC. One-shot circuits convert the CFD output (hit) signals from each channel, whose width depends on the APD signal's time over threshold, into fixed-width pulses to provide coincidence windows of well-defined widths. A logical OR of these pulses is distributed to other FREDA chips in the detector system via the IC's CORR_OUT output. The hit signals from these other chips are received through the CORR_IN input and brought into coincidence with the local hit signals, which are delayed to match the propagation delay of the incoming signals. The delay and coincidence width are digitally adjustable over wide ranges, common to all channels. For test purposes, the chip provides the options of external and singles triggering.

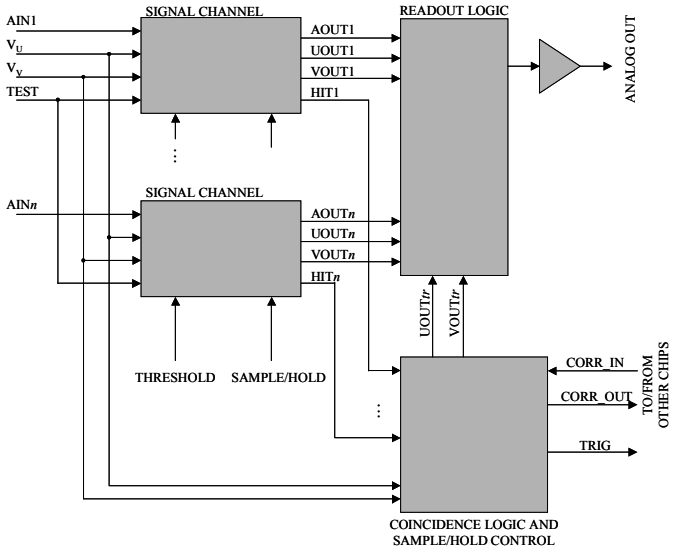

Fig. 1. Top-level block diagram of the FREDA IC.

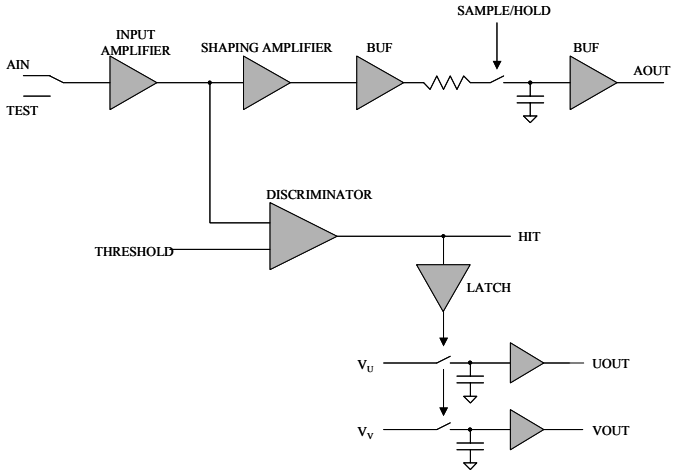

Fig. 2. Signal channel block diagram of the FREDA chip.

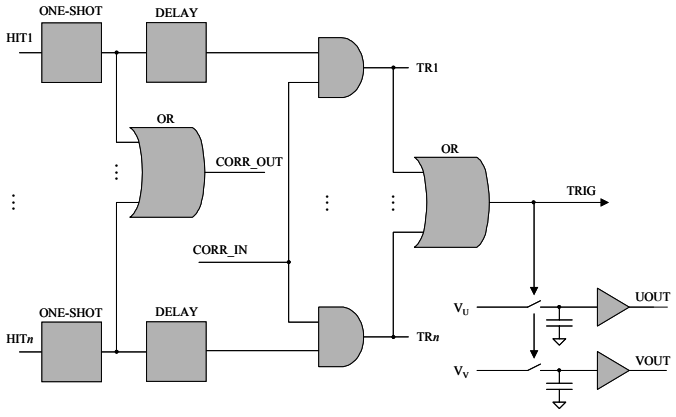

Fig. 3. Coincidence circuitry of the FREDA IC

The chip facilitates the recording of signal timing information by providing inputs for two user-supplied periodic "timestamp" signals (V_U and V_V in Fig. 2 and Fig. 3). On any channel, the values of these signals are latched in sample-and-hold (S/H) circuits each time that channel's CFD detects a hit; another pair of S/H circuits is latched whenever a coincidence

is detected. The timestamp values can be read out and digitized together with the pulse height signals and used to correct pulse-height dependent time walk or to tighten coincidence requirements in the offline analysis. By supplying the signals externally, the timing resolution and range can be optimized for each specific application, enhancing the versatility of the design. The channel timestamps are released automatically if the corresponding coincidence window expires before a coincidence is detected.

A number of configuration options, including different shaping times, facilitate flexible system design and promise to make the IC and detector module useful for a wide range of applications, beyond breast cancer imaging. Addressing one of the important design requirements described above, all chip circuits are designed to minimize power dissipation.

Fig. 4 shows the layout and pad assignments of the FREDA chip, which has been fabricated in a 0.35 μm process. The APD signal inputs are located along the two long edges of the die, arranged in groups of eight channels that are separated by wide ground bands for improved noise isolation. Bias and control signal pads are found along the short edges of the chip, with power supply pads in the corners. Fig. 5 shows a photograph of the chip mounted in a CQFP package. First comprehensive test results for the FREDA chip and the detector module are expected early in 2005.

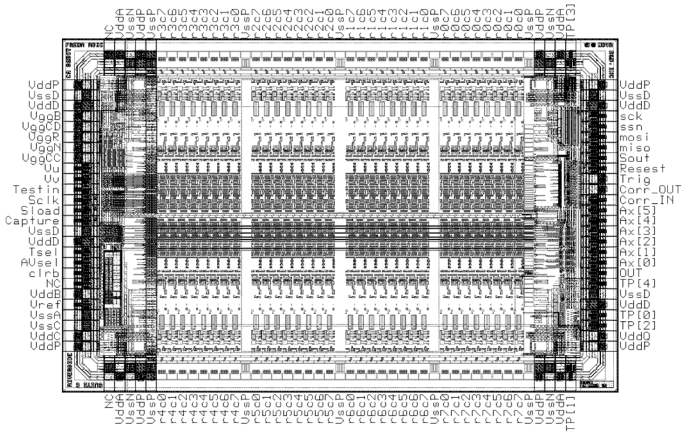

Fig. 4. Layout and pad assignments of the FREDA IC.

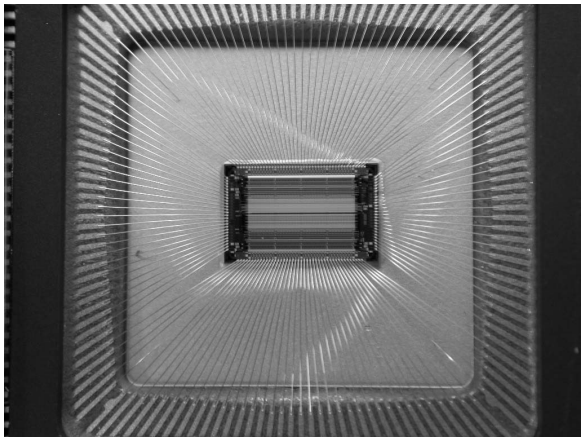

Fig. 5. Photograph of the FREDA chip mounted in a CQFP package

IV. Acknowledgments

We are grateful to Gerard Visser, Kanai Shah, and Richard Farrell for helpful discussions about the chip design requirements.

V. References

[1] American Cancer Society: Cancer Facts and Figures 2004; available at http://www.cancer. org/docroot/STT/stt_0.asp.

[2] I. Andersson et al., Mammographic screening and mortality from breast cancer: The Malmö mammographic screening trial. *Br. Med Journal* 297, 943 (1988).

[3] L.P. Adler, J.P. Crowe, N.K. Al-Kaisi, and J.L. Sunshine, Evaluation of breast masses and axillary lymph nodes with [F-18] 2-deoxy-2-fluoro-D-glucose PET. *Radiology* 187, 743 (1993).

[4] J.A. Glasby, R.A. Hawkins, C.K. Hoh, and M.E. Phelps, Use of positron emission tomography in oncology. *Oncology* 7, 41 (1993).

[5] R.R. Raylman, S. Majewski, R. Wojcik, A.G. Weisenberger, B. Kross, V. Popov, and H. Bishop. The potential role of positron emission mammography for detection of breast cancer. A phantom study. *Med. Physics* 27, 1943 (2000).

[6] C. J. Thompson et al., Positron Emission Mammography (PEM): A Promising Technique for Detecting Breast Cancer. *IEEE Trans. Nucl. Sci.*, 42, 1012 (1995).

[7] I. Weinberg et al., Preliminary Results for Positron Emission Mammography: Real-time Functional Breast Imaging in a Conventional Mammography Gantry. *Eur. Journal of Nuclear Medicine*, 23, 804 (1996).

[8] R. Freifelder and J. Karp, Dedicated PET Scanners for Breast Imaging. *Physics in Medicine and Biology*, 42, 2463(1997).

[9] G. Hutchins and A. Simon, Evaluation of Prototype Geometries for Breast Imaging with PET Radiopharmaceuticals. *Journal of Nuclear Medicine*, 36, 69P (1995).

[10] W.W. Moses, T.F. Budinger, R.H. Huesman, and S.E. Derenzo, PET Camera Designs for Imaging Breast Cancer and Axillary Node Involvement. *Journal of Nuclear Medicine*, 36, 69P (1995).

[11] N.K. Doshi, Y. Shao, R.W. Silverman, S.R. Cherry, Design and Evaluation of an LSO PET Detector for Breast Cancer Imaging. *Medical Physics*, 27, 1535 (2000).

[12] K.S. Shah, R. Farrell, R.F. Grazioso et al., Planar processed APDs and APD arrays for scintillation detection. *IEEE MIC conf. record*, Seattle, 1999.

[13] Y. Shao et al., Design studies of a high-resolution PET detector using APD arrays. *IEEE Trans. Nucl. Sci*. 42, 1051(2000).

[14] RMD, Inc., Watertown, MA, Silicon Avalanche Photodiodes: Specifications [Online]. http://www.rmdinc.com/production/apd.html.

[15] G. Visser, S. Cherry, M. Clajus, Y. Shao, and T.O. Tümer, Development of low power high speed readout electronics for high resolution PET imaging with LSO and avalanche photodiode arrays, *IEEE MIC conference record, San Diego, 2001.*